Particuology 57 (2021) 72–81

Contents lists available at ScienceDirect

Particuology

journal homepage: www.elsevier.com/locate/partic

Growth-controlled synthesis of polymer-coated colloidal-gold nanoparticles using electrospray-based chemical reduction

Mohamed Hasaan Hussain[a], Noor Fitrah Abu Bakar[a,*], Kim-Fatt Low[b], Ana Najwa Mustapa[a], Fatmawati Adam[c], Mohd Nazli Naim[d], I. Wuled Lenggoro[e,f]

[a] Faculty of Chemical Engineering, Universiti Teknologi MARA, Shah Alam, Selangor 40450, Malaysia
[b] Faculty of Applied Sciences, Universiti Teknologi MARA, Perak Branch, Tapah Campus, Tapah Road, Perak 35400, Malaysia
[c] Faculty of Chemical and Process Engineering Technology, Universiti Malaysia Pahang, Lebuh Raya Tun Razak, Gambang, Pahang 26300, Malaysia
[d] Department of Process and Food Engineering, Faculty of Engineering, Universiti Putra Malaysia, Serdang, Selangor 43400, Malaysia
[e] Graduate School of Bio-Applications and Systems Engineering, Tokyo University of Agriculture and Technology, Naka Cho, 2-24-16, Koganei, Tokyo 184-8588, Japan
[f] Department Chemical of Engineering, Tokyo University of Agriculture and Technology, Naka Cho, 2-24-16, Koganei, Tokyo 184-8588, Japan

ARTICLE INFO

Article history:
Received 27 July 2020
Received in revised form
16 November 2020
Accepted 2 December 2020
Available online 2 March 2021

Keywords:
Electrospray
Gold nanoparticles
Chemical reduction method
L-ascorbic acid
PVP
Aqueous medium

ABSTRACT

In this study, the controlled nucleation and growth of gold nanoparticles (GNPs) were investigated using a self-repelled mist in a liquid chemical reaction environment. An electrospray-based chemical reduction method was conducted in the aqueous region and at room temperature to synthesize the polymeric-stabilized gold nanoparticles. The electrospray technique was used to atomize a hydrogen tetrachlorourate (III) ($HAuCl_4$) precursor solution into electrostatically charged droplets. The atomized droplets were dispersed in an aqueous reaction bath containing L-ascorbic acid as a reducing agent and polyvinylpyrrolidone (PVP) as a stabilizer. The effect of the electrospray parameters, specifically the flow rate and electrospray droplet size, as well as the reaction conditions such as the concentration of reactants, pH, and stabilizer (PVP), were investigated. The mean diameter of the GNPs increased from around 4 to 9 nm with an increase in the electrospray flow rate, droplet size, and current passing through the electrospray jet. Spherical and monodispersed GNPs were synthesized at a relatively high flow rate of 2 mL/h and a moderate concentration of 2 mM of precursor solution. The smallest-sized GNP with a high monodispersity was obtained in the reaction bath at a high pH of 10.5 and in the presence of PVP. It is expected that continuous and mass production of the engineered GNPs and other noble metal nanoparticles could be established for scaling up nanoparticle production via the proposed electrospray-based chemical reduction method.

Introduction

The demand for GNPs has dramatically increased owing to their versatile optical and electrochemical properties that can be utilized effectively in various applications such as medical diagnosis (Dykman & Khlebtsov, 2011; Yeh et al., 2012), therapeutic (Sztandera et al., 2019), catalyst (Stratakis & Garcia, 2012; Thompson, 2007), and electronic applications (Homberger & Simon, 2010). Uniquely, the inherent optical and electrochemical traits of GNPs are governed by their size, morphology, and crystallinity (Alex & Tiwari, 2015; Amendola et al., 2017). Therefore, more attention has been given to the synthesizing or tailoring of GNPs with desirable properties. Fundamentally, GNP synthesis methods can be classified into either physical or chemical types. Generally, physical synthesis methods are high-energy processes in which the high-energy environment prevents the functionalization of nanoparticles with ligands. In addition, it is very difficult to fine tune the size and morphology of the GNPs when using physical methods (Mafuné et al., 2001). Conversely, bottom-up methods such as chemical synthesis have been found to be promising because of their simplicity, low energy requirements, and ability to conjugate with any ligand.

The reduction of gold(III) chloride using mild reducing agents such as in the case of the citrate method proposed by Turkevich (Kimling et al., 2006) or organic solvents using the two-phase synthesis method proposed by Brust and Scriffin (Brust et al., 2000)

* Corresponding author.
E-mail address: fitrah@uitm.edu.my (N.F. Abu Bakar).

https://doi.org/10.1016/j.partic.2020.12.004

are the most widely used GNP chemical synthesis methods. Among these, the Turkevich method is recognized as being the best choice for synthesizing GNPs in a green reagent because of its simple, single-step process, fast synthesis time, and support of the use of a wide range of reducing agents. Despite these advantages, the pH, temperature, and molar ratio of the reactants must be strictly observed to control the properties of the GNPs produced using this method (Tran et al., 2016; Tyagi et al., 2016). The Brust method is preferred for synthesizing gold seeds because of its fast reaction ability. However, its use of non-green reducing agents such as $NaBH_4$ and organic solvent media do not allow it to be applied to the production of gold seeds in biological applications, and the two-phase process associated with this method requires additional effort (Brust et al., 1994). Conversely, the optimization of the properties of colloidal nanoparticles by choosing a suitable method for adding and mixing reactants (such as drop by drop, continuous flow addition, and spraying methods) has received considerable attention. Classical nucleation theory (CNT) points to the reaction rate of reactants and the concentration of solutes determining the nucleation and growth of nanoparticles in the colloidal solution (Thanh et al., 2014). Supporting this fact, related studies have proven that the reactant distribution method and mixing efficiency considerably influence the particle size (Pacławski et al., 2011; Sugano et al., 2010). In particular, the distribution and mixing of reactants can be efficiently controlled by the application of electrospray technology to GNP synthesis.

The electrospray technique involves the breaking up of fluids into mist particles by applying an electric field. In the electrospray process, a high-voltage electric field is applied to the meniscus of a continuously flowing fluid such that it is monodispersed and a few nanometric-to-micrometric self-repelled droplets are generated due to coulombic fission (Gomez & Tang, 1994; Smith, 1986).This technique consumes less energy for aerosol generation than other conventional atomization techniques such as arc discharge, laser ablation, pyrolysis, and chemical vapor deposition methods. Currently, this versatile technique is utilized in many nanomanufacturing applications such as nanoparticle coating Halimi et al., 2014), nanocomposite synthesis (Halimi et al., 2018; Naim et al., 2015), bionanomaterial preparations (Zolkepali et al., 2014), drug delivery (Ramakrishna & Sreedar, 2013; Zolkepali et al., 2018), and characterization techniques (Lenggoro et al., 2002). Previously, colloidal GNP synthesis using the electrospray method produced anisotropic GNPs (Quintanilla et al., 2010; Soliwoda et al., 2015). However, these anisotropic GNPs were produced in the presence of toxic organic reducing agents such as dodecylaminomethanol (DDAM) and octadecylaminomethanol (ODAM), as well as solvents such as formaldehyde (FA) and cyclohexane. Furthermore, the mechanism of GNP formation in the electrospray method and the correlation between the electrospray parameters and GNP properties were not addressed in detail by these studies.

In this study, we developed an electrospray system that incorporates the Turkevich method to produce size-controlled and monodispersed GNP seeds. Gold nanoseeds were successfully produced in an aqueous medium using a green reducing agent instead of toxic chemicals (such as $NaBH_4$) and organic solvents, which may allow these particles to be used in biological applications. In addition, this study proposes a novel strategy for optimizing the size of the gold nanoparticles by manipulating the electrospray parameters (such as the flow rate and precursor solution conductivity) rather than the reaction conditions (such as the pH and reactant concentration). Briefly, the Au^{3+} precursor solution was transformed to a mist of micro- and nanoscale droplets by an electrospray process. The mist was incorporated into the reaction bath containing H_2O, L-ascorbic acid, and PVP as a green stabilizer. In this mist-to-liquid reaction environment, uniform mass transfer was achieved, as was the homogenous nucleation and growth of GNPs. Using this method, we should be able to produce gold nanoseeds of a controlled size by simply manipulating the size, concentration, and size uniformity of the electrospray precursor droplets.

Materials and methodology

Materials

Hydrogen tetrachloraurate (III) ($HAuCl_4{\cdot}3H_2O$, ≥ 99% trace metal basis) $HAuCl_4{\cdot}3H_2O$, PVP K30 (MW ~ 40 000), and crystalline L-ascorbic acid (reagent grade) were purchased from Sigma Aldrich, Malaysia. Ethanol (99.85% assay) and ethylene glycol (99.5% assay) were obtained from Merck-Chemicals.

Electrospray precursor solution preparation

The gold precursor was prepared in three batches of different concentrations, namely, 1, 2, and 4 mM by adding $HAuCl_4$ trace metal solution to an 80 vol.% ethanol and 20 vol.% ethylene glycol solvent mixture. The $HAuCl_4$ was dissolved in an ethanol/ethylene glycol solvent mixture and then electrosprayed into a 24-mL reaction bath containing an aqueous L-ascorbic acid solution. Note that the volume of the sprayed precursor solvent (ethanol/ethylene glycol) is smaller than the volume of aqueous reducing agent solution. Therefore, the effect of the presence of organic solvent impurities inside the aqueous reaction bath can be neglected.

One of the novelties of this study was the synthesis of GNPs in aqueous solvents using the electrospray technique. However, water could not be used as a solvent for the electrospray precursor because of its high surface tension and conductivity. In practice, fluids with a conductivity in the range of 10^{-4} Sm^{-1} to 10^{-8} Sm^{-1} and a surface tension of less than 5×10^{-2} Nm^{-1} were preferred for use as a suitable solvent for electrospray applications. If the conductivity of the precursor liquid exceeds this range, the electrical current passing through the electrospray jet increases and hinders the electrospray (Barrero & Loscertales, 2007; Fernández de la Mora, 2007). Similarly, it is necessary to apply a high level of electrical energy to produce electrospray droplets from liquids having a high surface tension (Smith, 1986). Hence, liquids with a high conductivity and high surface tension generate a corona discharge that leads to the production of large electrospray droplets. Unfortunately, this phenomenon is often associated with the use of an aqueous solvent, which has a surface tension and electrical conductivity of 73×10^{-2} Nm^{-1} and $\geq 10^{-6}$ Sm^{-1}, respectively. Therefore, an 80% v/v ethanol/20% v/v ethylene glycol mixture was used as the optimal precursor solvent for the electrospray process.

Reducing agent preparation

Two batches of reducing agent streams were prepared. In the first batch, L-ascorbic acid crystals were dissolved in distilled water to make 24 mL of 2.5 mM L-ascorbic acid aqueous solution. In the second batch, 24 mL of 2.5 mM L-ascorbic solution with 1% w/v PVP was prepared by dissolving L-ascorbic acid crystal along with PVP K30 polymer in distilled water. According to the experimental requirements, the pH of the PVP-added reaction baths was adjusted to 3.5 and 10.5 by adding concentrated $NaOH_{(aq)}/HCl_{(aq)}$. All the solutions were stirred at 800 rpm for 2 h at room temperature (25–28 °C) to obtain a uniform solution.

Experimental setup of electrospray system and reaction bath

A typical instrument setup for the electrospray synthesis of colloidal GNPs was fabricated with a high-voltage power supply, syringe pump, 5-mL plastic syringe, 3-mm diameter plastic hose, and 23-G metal nozzle, as depicted in Fig. 1. In the electrospray

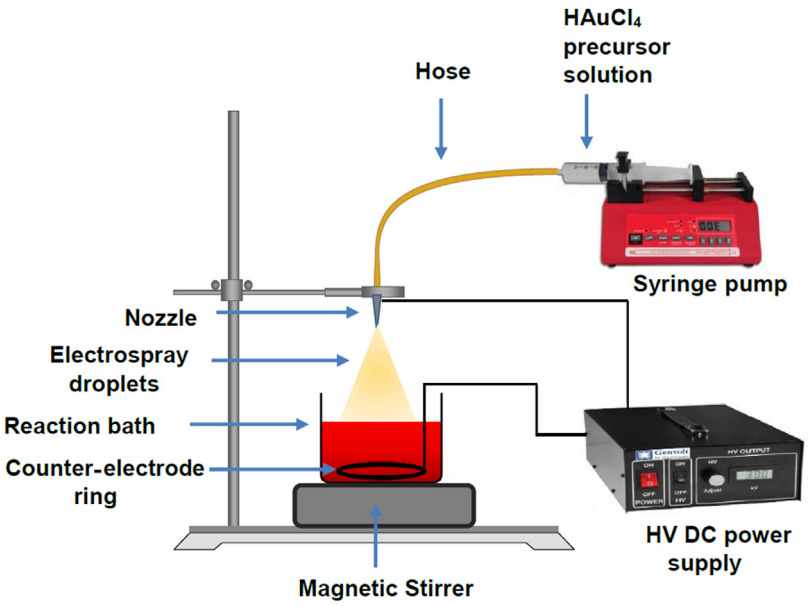

Fig. 1. Electrospray-based chemical reduction system for GNP synthesis.

setup, the syringe pump was used to pump the precursor solution in the reaction bath through the capillary at a constant flow rate. In each experiment, the 5-mL plastic syringe was filled with the required volume of precursor solution ($HAuCl_4$ organic solvent solution) and fixed onto the syringe pump. The outlet of the syringe pump was connected to the fine tube with the stainless-steel nozzle at the other end. The nozzle was coupled to the high-voltage power supply, while a counter-electrode ring was placed in the reaction bath. The reaction bath (droplet collector) consisted of the reducing agent, counter-electrode (Sn-Pb metal ring), Polytetrafluoroethylene (PTFE)-coated magnetic stirrer, and a beaker. The beaker was placed directly under the electrospray nozzle, and the distance between the nozzle orifice and the surface of the reducing solution was maintained at 10 mm. The counter-electrode ring was immersed in the reducing agent at the bottom of the reaction bath. The PTFE-coated magnet was placed in the reaction bath and used to stir the bath at 300 rpm.

During the electrospray process, the precursor solution was pumped through the electrified capillary nozzle at flow rates of 0.5, 1, and 2 mL/h. The high-voltage power supply, applied to the nozzle, was adjusted from 0 to 11.5 kV. The high voltage difference caused an electric field to be induced between the nozzle and grounded counter electrode. This electric field causes the precursor droplets to be atomized into much smaller droplets, followed by aerosol formation. The experiment duration was determined based on the flow rate and concentration of the precursor solution. In each experiment, the 6 μmol Au^{3+} precursor was electrosprayed to obtain the same amount of GNP product. The molar ratio of L-ascorbic acid to gold(III) chloride was maintained at 1:10. The flow rate and concentration of the precursor solution were considered as the main variables of the GNP synthesis. The experiment was carried out at room temperature (25 °C).

Characterizations

The size and morphology of the synthesized GNPs were analyzed using a Tecnai G2 20 Twin transmission electron microscope (TEM). An Agilent Cary 60 UV–vis spectrophotometer was used to investigate the plasmon resonance of the GNP colloids. Furthermore, the mean particle diameter, particle size distribution, and zeta potential of the GNPs were analyzed by dynamic light scattering (DLS) using a Malvern Zetasizer Nano ZS.

Governing equations

Eqs. (1)–(3) were used to determine the electrospray primary droplet size, the current passing through the jet, and the secondary droplet (droplet size after coulombic fission) size, respectively. The Au^{3+} metal ion solution, which has high conductivity, was used as the electrospray precursor. During the electrospraying of the highly conductive liquid, the high flow rate and high surface tension increased the current passing through the jet. The high current flow enhanced the high electric stresses on the jet and resulted in the wiping mode of the jet breakup. The primary droplet size and current passing through the wiping mode jet can be determined by applying Hartman's cone-jet mode equations (Hartman et al., 2000). We assume that the real values of the electrospray droplet size (d_d) and current (I) in this study were less than the calculated values given by Eqs. (1) and (2).

$$d_d = \left[0.8\left(\frac{288\varepsilon_o\gamma Q^2}{I^2}\right)\right]^{1/3}, \tag{1}$$

$$I = 2(\gamma k Q)^{1/2}, \tag{2}$$

where γ is the surface tension of the precursor solution (27×10^{-3} N/m), k is the electrical conductivity of the precursor solution (0.013 S/m, 0.025 S/m, and 0.049 S/m for 1, 2, and 4 mM concentrations of Au^{3+} ion solution), ε_o is the permittivity of free space (8.854×10^{-12} CV^{-1} m^{-1}), Q is the flow rate (m^3/s), which was a manipulating parameter as explained earlier.

The theoretical value of the secondary droplet size (droplet size after coulomb fission) (d_s) of the electrospray can be calculated using Eq. (3) (Hogan et al., 2007), assuming no mass loss during the electrospray droplet formation.

$$d_s = d_d\varphi^{1/3}, \tag{3}$$

where d_d is the primary droplet size of the particles produced by the electrospray obtained from Eq. (1) and φ is the volume fraction of $HAuCl_4$ in the precursor solution.

The mean particle size and polydispersity index (PDI) of the particles were determined from the number distribution (number PSD)

and intensity distribution (intensity PSD) DLS results, respectively. For all the electrospray samples, a higher number distribution of smaller-sized GNPs and a lower number distribution of very large AuNPs were obtained. The secondary larger size distribution of the GNPs was obtained owing to the continuous synthesis that caused seed-mediated growth. However, a small number of very large particles can be removed from the sample by using either nanopore filter paper or centrifuging (Soliwoda et al., 2015). Therefore, the PDI of the individual peak that represents the group with the highest number of particles (≥95 number %) in the number distribution graph was calculated using Eq. (4):

$$\mathrm{PDI} = (\mathrm{standarddeviation}/\mathrm{meanparticlesize})^2 \quad (4)$$

Results and discussion

After the precursor solution was electrosprayed from the nozzle, discrete tiny droplets were driven into the reaction bath containing L-ascorbic acid with PVP. The electrosprayed droplets that contained Au^{3+} were dispersed into the reducing agent region and reacted with the L-ascorbic acid. The chemical reaction for Au^0 formation is given by Eq. (5):

$$2AuCl_4^- + 3C_6H_8O_6\,(\mathrm{ascorbic\ acid}) \rightarrow 2Au^0 + 3C_6H_6O_6\,(\mathrm{dehydroascorbic\ acid}) + 8Cl^- + 6H^+ \quad (5)$$

During the electrospray process, the discrete electrospray precursor droplets were dispersed in the reaction bath containing a reducing agent (L-ascorbic acid molecules) and stabilizer molecules (PVP). After the reduction of the Au^{3+} ions by the L-ascorbic acid, Au solutes were formed, followed by particle growth. In the growth stage, the particle size was controlled by the stabilizer molecules. It was hypothesized that, when the Au^{3+} ion-containing self-repelled electrospray droplets were incorporated into the reaction bath, they created a detached and isolated environment for the nucleation and growth of GNPs in the solution. This discrete reaction area was limited by the size and metal-ion concentration of the electrospray droplets.

Influence of flow rate

Fig. 2 shows the TEM images of the electrospray-synthesized GNPs at three different flow rates. Electrosprayed GNPs with average diameters of 8.6 ± 4.2, 4.8 ± 1.5, and 3.7 ± 1.7 nm were obtained from flow rates of 0.5, 1, and 2 mL/h, respectively. These results indicate that the sizes of the GNPs decrease with an increase in the flow rate. At a low flow rate, the relaxation time of the precursor solution inside the electrified capillary is longer. This long relaxation time of the capillary fluid allows a high surface charge to be induced on the electrosprayed droplets, such that the droplets are greatly repelled in the plume region, yielding small droplets. In addition, droplets produced from a low flow rate take a long time to reach the reaction bath, such that there is more time for the solvent to evaporate from the droplets. Eventually, the electrosprayed droplets shrink, and smaller droplets are produced (Wortmann et al., 2007). Therefore, the low flow rate of the precursor Au^{3+} solution produced small droplets that led to the production of larger GNPs, whereas the opposite was observed in the case of a high flow rate.

Fig. 3(a) shows the impact of the droplet size (determined by Eq. (3)) on the size of the synthesized GNPs (as measured using TEM). The graph shows that 8.6 ± 4.2-, 4.8 ± 1.5-, and 3.7 ± 1.7-nm GNPs were produced from droplets with estimated sizes of 205, 348.5, and 451 nm, respectively. Small GNPs were produced from relatively large electrospray droplets, and relatively large GNPs were produced from smaller electrospray droplets. When the concentration of the precursor solution is a constant parameter, the smaller electrospray droplets carry a smaller amount of Au^{3+} ions to the reaction bath. This low distribution rate of Au^{3+} ions results in a low Au solute concentration that takes a long time to reach the supersaturation level for burst nucleation in the reaction bath. In agreement with classical nucleation theory, the growth rate of the GNPs could be controlled over the nucleation rate of Au monomers at lower flow rates such that larger nanoparticles were obtained (Zong et al., 2014b; Lince et al., 2008). Conversely, a large amount of Au^{3+} ions was carried by the large droplets produced by the high flow rate. Thus, the nucleation rate of Au monomers dominates the growth rate and smaller GNPs are produced at a high flow rate (Luo et al., 2015). In addition, considerable time is needed to spray the whole precursor solution at a low flow rate. Therefore, when the precursor (Au^{3+}) droplets are added slowly and continuously to the reaction bath, the electrosprayed Au^{3+} ions can cause heterogeneous nucleation and trigger seed-mediated growth that leads to the formation of large GNPs at lower flow rates, as depicted in Fig. 3(b). Similar phenomena have been observed in continuous-flow reactors, as designed by other researchers (Bandulasena et al., 2017; Lohse et al., 2013).

Fig. 4(a) shows the hydrodynamic mean diameters and size distributions of the synthesized GNPs, which were characterized using the DLS technique. These results show that GNPs with mean diameters of 6.8 ± 1.6, 7.5 ± 2.2, and 11.7 ± 3.5 nm were obtained with electrospray flow rates of 2, 1, and 0.5 mL/h, respectively. Moreover, they indicate that the hydrodynamic mean diameter of the GNPs increased as the flow rate decreased. The PDI values obtained by DLS measurements were 0.07, 0.09, and 0.26 for flow rates of 2, 1, and 0.5 mL/h, respectively. These values increased as the flow rate of Au^{3+} decreased, indicating that the slow addition of the precursor solution (low flow rate) resulted in polydisperse particles. At lower flow rates, the continuous growth and seed-mediated growth of GNPs increases the chance of the formation of particles of heterogeneous sizes (Zong et al., 2014a). Fig. 4(b) shows the UV–vis absorbance spectra of the synthesized GNPs for different flow rates of precursor solution. It is known that UV–vis absorbance spectra in the range 520–600 nm with a single maximum absorbance peak (λ_m) imply the presence of GNPs in the colloidal solution (Haiss et al., 2007). The obtained λ_m for GNPs at flow rates of 2, 1, and 0.5 mL/h were 519, 523, and 530 nm, respectively, which is consistent with the increase in the average particle diameter observed by previous TEM and DLS measurements.

It is important to note that, although the TEM and DLS results exhibit the same trend in every experiment, the TEM-determined mean particle diameters were consistently smaller than the DLS-determined mean particle diameters. This difference between the two methods is attributed to the hydrodynamic diameter, which is determined using the DLS method. When GNPs are protected by PVP polymer layers, DLS measurements obtain the total reflection of the center of the GNPs and hydrated PVP polymer shells in the colloidal solution. Conversely, TEM measurements only probe the electron-rich inner core of the particle, such that the determined values are smaller than the DLS measurements.

Concentration of Au^{3+} ions in precursor solution

Fig. 5 shows the UV–vis absorbance spectra of the AuNPs synthesized from various concentrations of precursor solution (Au^{3+} ion concentration). The results show that λ_m is observed at 529, 519, and 520 nm for the GNPs synthesized at precursor concentrations of 1, 2, and 4 mM, respectively. Overall, the λ_m obtained from 2 and 4 mM precursor solutions indicated the presence of smaller AuNPs in a high concentration of electrospray precursor, whereas the highest λ_m obtained from GNPs produced by the 1 mM precursor imply the presence of the largest particles. In the electrospray process, the

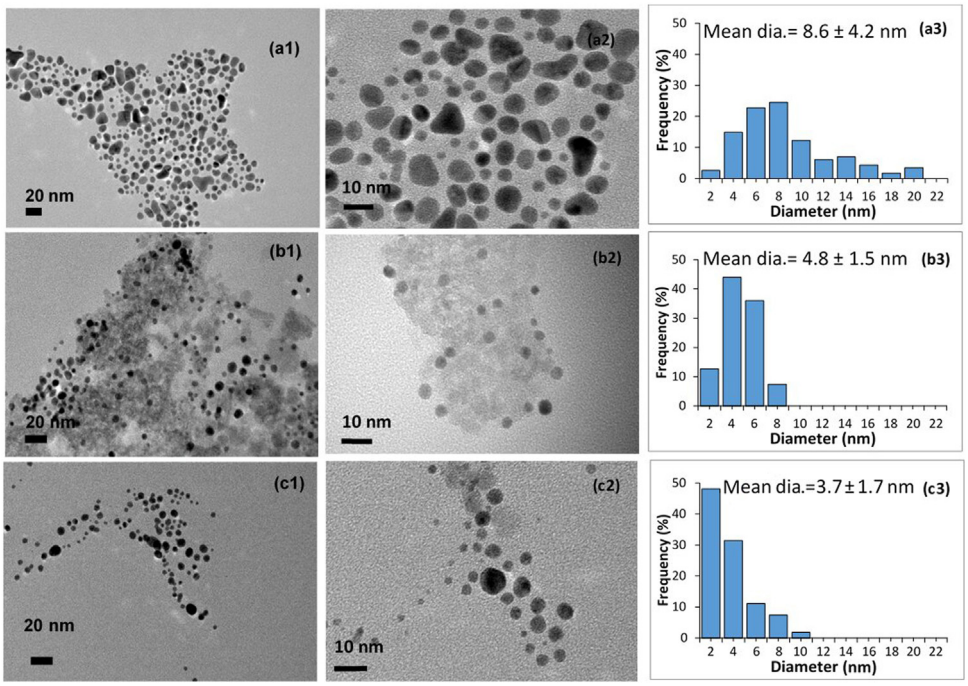

Fig. 2. TEM micrographs and size distribution of GNPs for flow rates (a1, a2) and (a3) 0.5 mL/h, (b1, b2) and (b3) 1 mL/h, and (c1, c2) and (c2) 2 mL/h.

Table 1
Size measurements of GNPs with increasing concentrations of Au^{3+} and current flow through the Taylor cone jet.

Concentration of Au^{3+} precursor (mM)	Current through Taylor cone (μA)	Hydrodynamic mean diameter (nm)	Polydispersity index (PDI)
1	0.87	11.2 ± 2.3	0.05
2	1.23	6.8 ± 1.6	0.07
4	1.72	6.7 ± 1.8	0.2

current passing through the jet increases with the conductivity (k) of the precursor solution, where the conductivity is proportional to the metal-ion concentration of the precursor (see Eq. (2) and Table 1). However, according to Eq. (1), the electrospray diameter is inversely proportional to I^2. Therefore, smaller electrospray droplets were produced with precursors having a high Au^{3+} concentration. Although these droplets were relatively smaller than those produced at low concentrations, the high Au^{3+} ion content led to a high nucleation rate, resulting in a small particle size.

Table 1 lists the mean hydrodynamic diameter of the GNPs obtained using DLS. It was found that particles measuring 11.2 ± 2.3, 6.8 ± 1.6, and 6.7 ± 1.8 nm were produced from precursor solutions of 1, 2, and 4 mM, respectively. DLS measurements showed that the mean hydrodynamic particle diameter was smaller for a precursor with a relatively high concentration of Au^{3+}. These results are in agreement with the previous discussion, that is, the slow nucleation of particles followed by fast GNP growth resulted in larger particles in the case of a precursor with a low concentration of Au^{3+}. However, the PDI of GNPs synthesized by 1, 2, and 4 mM Au^{3+} were 0.07, 0.07, and 0.2, respectively. This trend shows that the highest concentration of 4 mM produced highly polydisperse particles. In this study, the electrospray reactor system was designed as a semi-batch reactor. Therefore, during the continuous distribution of the precursor solution, the particles that formed earlier were retained in suspension and could have stimulated seed-mediated growth of upcoming Au^{3+} ions, thus resulting in the formation of polydisperse particles.

From another aspect, the conductivity of the precursor solution is one of the dominant parameters that governs the electrospray process. The correlation between the conductivity (k) of the precursor solution and the current passing through the electrospray cone (I) is given by Eq. (2), where k is proportional to I. In addition, Table 1 indicates that I increases (from 0.87 to 1.72 μA) with an increase in the concentration of the Au^{3+} metal ions (from 1 to 4 mM). Furthermore, when the Au^{3+} precursor concentration exceeded the limit of 2 mM, the electrospray was hindered, with the formation of large electrospray droplets being observed. This was caused by the varicose instability of the electrospray jet, which emits an excessive electric charge due to the high metal concentration (Fernández de la Mora, 2007; Hartman et al., 2000; Rosell-Llompart & Fernández de la Mora, 1994). This unstable electrospray with a high-concentration precursor solution (4 mM) might create a non-uniform reaction environment and result in the formation of highly polydisperse particles.

Effect of stabilizing agent

In the present study, PVP was added as a stabilizer to control the growth of GNPs. Fig. 6(a) shows TEM images of the PVP-stabilized GNPs produced by the electrospray method. These images indicate that anisotropic and very small (mean diameter: 3.7 ± 1.7 nm) GNPs were produced in the presence of PVP molecules, whereas relatively large (mean diameter: 8 ± 3.4 nm) and polydisperse GNPs were obtained in the absence of the PVP molecules.

These results prove that the PVP polymer efficiently prevented particle growth and aggregation. In addition, a similar study proved that the addition of 1% w/v PVP is capable of stabilizing GNPs effectively by depletion stabilization (Bandulasena et al., 2017). PVP is an amphiphilic molecule with a hydrophobic pyrrolidine repeating unit that consists of a C=O carbonyl group and N species and a hydrophobic alkyl chain. When PVP is dissolved in a solvent, its highly polar C=O and =N groups, which are attached to the pyrrolidine ring, couple with the H_2O molecules via hydrogen bonds, whereas the rest of the apolar alkyl backbone chain exhibits considerable hydrophobicity (Dhumale et al., 2012; Hoppe

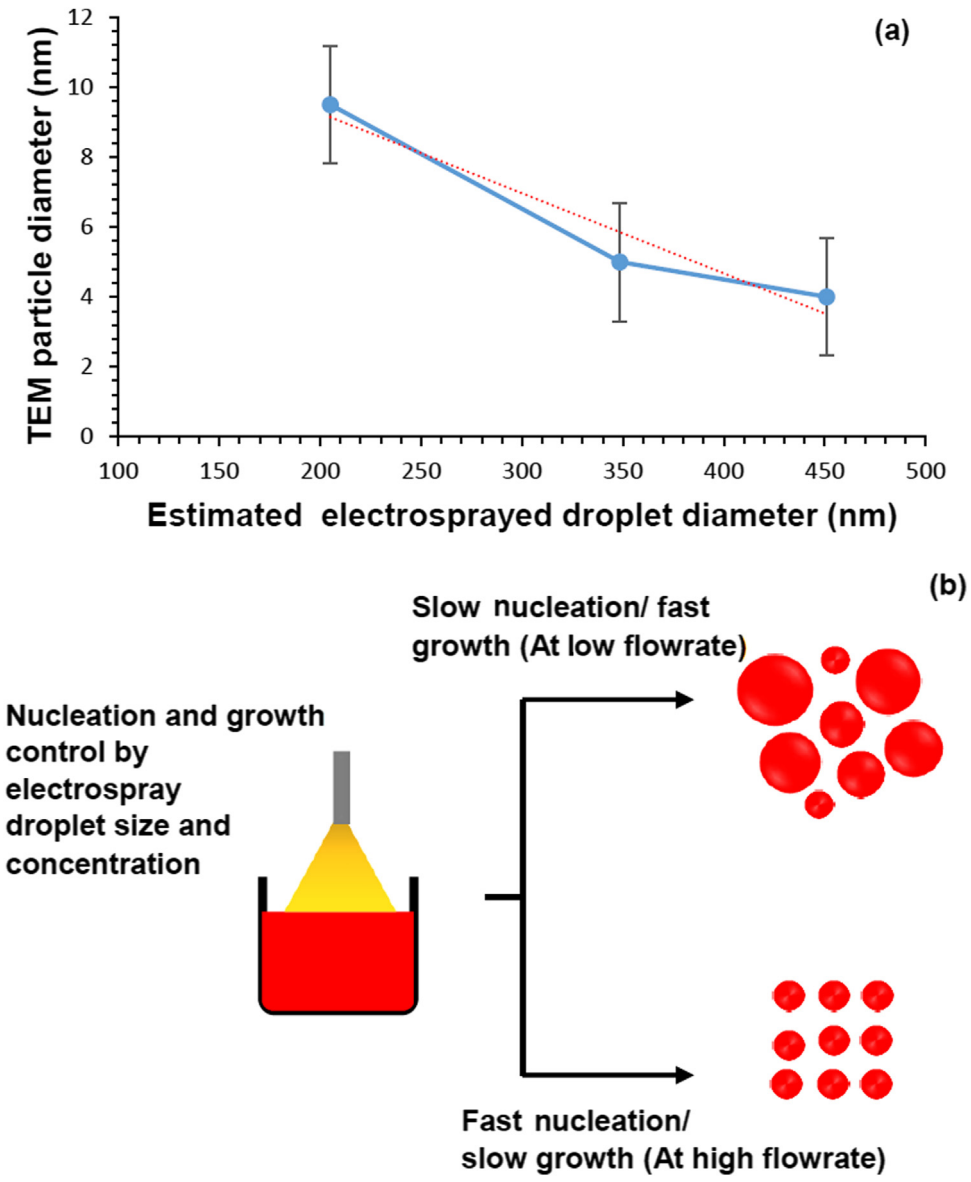

Fig. 3. (a) Experimental GNP particle diameters as observed by TEM vs. estimated droplet size estimated from Eq. (3) at different flow rates and (b) nucleation and growth of GNPs in electrospray process.

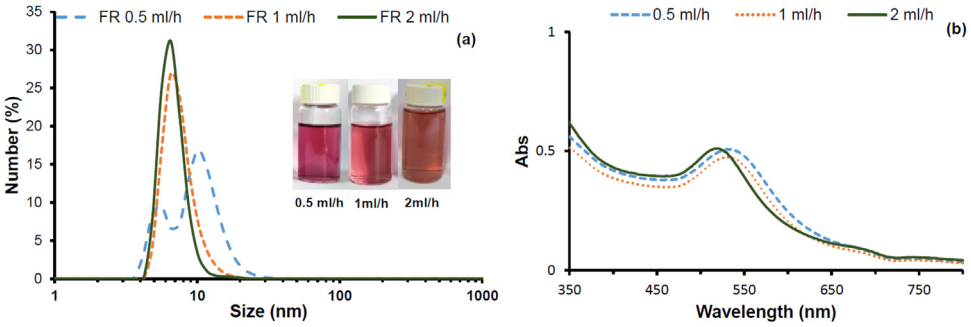

Fig. 4. (a) DLS size distribution of GNPs synthesized at different flow rates and (b) UV–vis spectra of GNPs synthesized at different flow rates.

et al., 2006; Papp et al., 2007). In the presence of GNPs, the C=O group of PVP attached to the metal nanoparticle surface adsorbs and the hydrophobic tail of the PVP extends in the solvent. These elongated hydrophobic alkyl chains interact with each other (by the steric repulsion mechanism) and prevent the agglomeration of GNPs (Papp et al., 2007). In related works, it was found that a 1% w/v PVP concentration is sufficient for stabilizing GNPs by depletion stabilization. Furthermore, in the present study, it was found that around 4-nm discrete GNPs were obtained with a 1% w/v PVP solution.

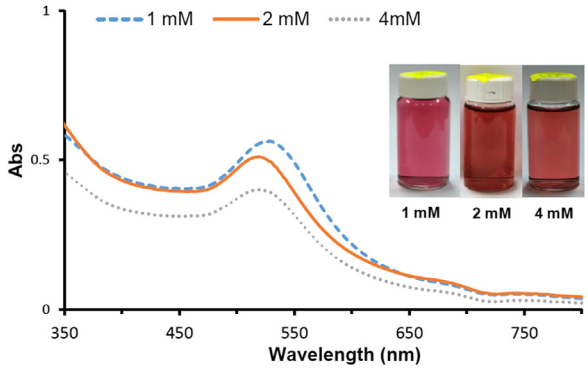

Fig. 5. UV–vis spectra of GNPs produced with different concentrations of precursor solution.

The TEM images in Fig. 6(b) show that monodispersed (spherical and quasi-spherical) GNPs were produced without PVP. These results point to the electrospray process being capable of producing GNPs by chemical reduction, whereby L-ascorbic acid reduces and stabilizes the GNPs. The molar ratio of ascorbic acid to Au^{3+} was 20:1 in the reaction bath, but the reaction stoichiometry of the L-ascorbic acid to Au^{3+} was 3:2. Therefore, this excessive amount of L-ascorbic acid in the reaction bath could also act as a stabilizing agent (Malassis et al., 2016). The carboxylic group of the dehydroascorbic acid molecules binds to the surface of the GNP surface and prevents the further growth and agglomeration of the GNPs by means of steric stabilization (D'Souza et al., 2014; Malassis et al., 2016). However, the affinity of the PVP to GNPs is stronger and more stable than that of the L-ascorbic acid–GNP counterparts because the TEM diameter of PVP-stabilized GNPs (mean diameter of 4 nm, see Fig. 6(a)) is smaller than that of the L-ascorbic acid-stabilized GNPs (mean diameter of 8.6 nm, see Fig. 6(b)).

Fig. 7(a) shows the UV–vis absorbance spectrum of GNPs with and without PVP, which were synthesized using electrospray. A small λ_m (approximately 519 nm) was obtained for PVP-stabilized GNPs and this peak shifted to a high wavelength of 528 nm for GNPs without PVP. In addition, the narrow UV–vis spectrum of the PVP-stabilized GNPs and the wide UV–vis spectrum of the non-PVP-stabilized GNPs indicated that the size distribution of the PVP-stabilized GNPs was narrower than that without PVP. Further quantitative analysis, measured using DLS as shown in Fig. 7(b), ensures that the mean hydrodynamic size of electrosprayed GNPs without PVP is 12.8 nm, which is double the size of the PVP-stabilized samples, i.e., 6.8 nm. Moreover, the PDI values of the PVP-stabilized GNPs (0.07) are lower than that of the electrosprayed GNPs without PVP (0.14). These results indicate that the particle sizes were uniform and homogenous as a result of adding PVP to the reaction bath during the electrospray process. The UV–vis spectra and DLS results are consistent with the TEM images and ensure that the PVP efficiently binds with the electrosprayed GNPs and controls the particle size and its distribution in the electrospray process.

Table 2
DLS size measurements of GNPs and redox potential of L-ascorbic acid.

pH of the L-ascorbic acid solution	Redox potential of the L-ascorbic acid solution (mV)	Hydrodynamic diameter of GNPs (nm)	PDI
3.5	+220	43.4 ± 20.6	0.5
10.5	−166	6.8 ± 1.6	0.07

Fig. 8 shows the UV–vis spectra and colors of GNPs that were synthesized at different redox potentials and pH values of the L-ascorbic acid solution (reducing agent). The UV–vis λ_m band of the GNPs, which was synthesized at a higher pH (10.5), shifted to a shorter wavelength relative to that of the AuNPs synthesized in L-ascorbic acid solution with a lower pH value (pH 3.5).

Fig. 9 shows the DLS size distribution patterns of those GNPs produced at reducing agent pH values of 3.5 and 10.5. The quantitative results obtained from DLS characterization with the pH and redox potential values of the reducing agents are listed in Table 2. These results show that those GNPs having a relatively large size

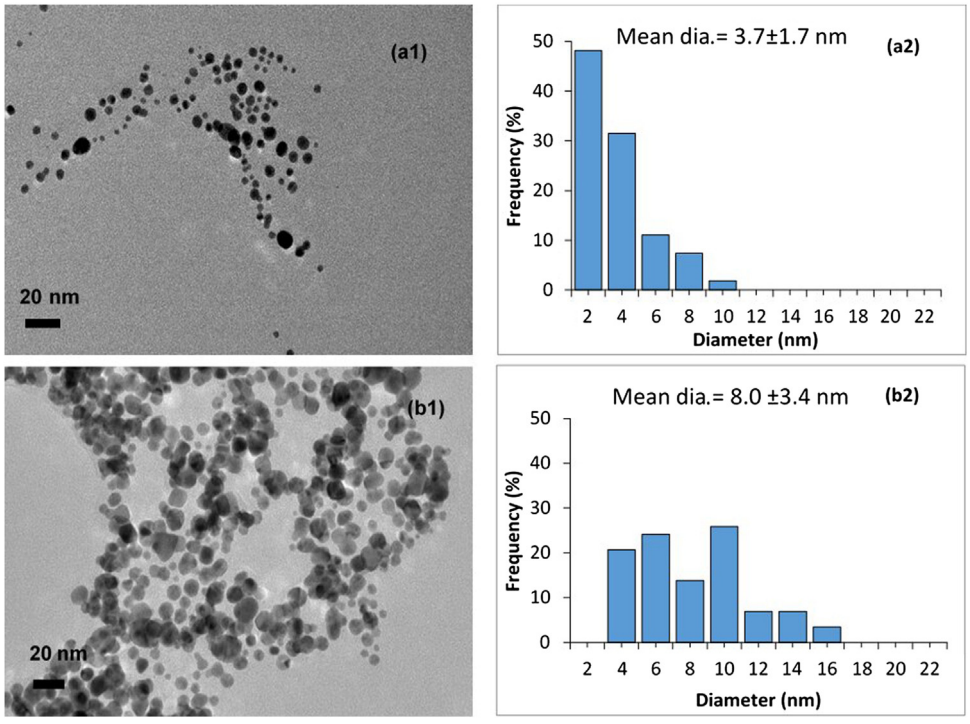

Fig. 6. TEM images and size distribution of electrosprayed GNPs (a1 and a2) with PVP and (b1 and b2) without PVP.

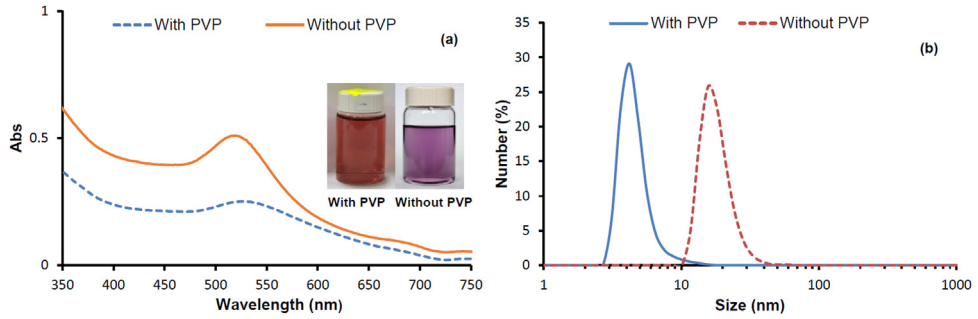

Fig. 7. (a) UV–vis spectra of electrosprayed GNPs with and without PVP and (b) DLS size distribution plot of electrosprayed GNPs with and without PVP.

of 43.4 nm were synthesized in an L-ascorbic acid solution with a low pH value of around 3.5 and a redox potential of +220 mV, while the particle size fell rapidly to 6.8 nm at a high pH value of around 10.5 and redox potential of −166 mV. In addition, the PDI values for those GNPs synthesized in the L-ascorbic acid solution at pH 10.5 was very low (0.07) relative to those of AuNPs synthesized in L-ascorbic acid with a low pH value of around 3.5 (0.5). These results indicate that monodispersed GNPs were synthesized at high pH values, whereas highly polydisperse GNPs were produced at lower pH values. When the pH of the L- ascorbic acid was > pH 10, the solution was dominated by AsH– species owing to the higher pK_a value (around 11.8). This AsH– species has a very strong reducing power, which results in a faster redox reaction and the formation of smaller GNPs. L-ascorbic acid is a dibasic soft acid. In aqueous solution, it can deprotonate due to hydrolysis by three different species: ascorbic acid (AsH_2), the ascorbate monoanion (AsH–), and the ascorbate di anion (As^{2-}) (Mukai et al., 1991). This deprotonation reaction is governed by the pH of the overall solution. The hydrolysis reaction of L-ascorbic acid in the equilibrium stage is defined by Eqs. (6) and (7),

$$AsH_2\,(\text{ascorbic acid})\; pK_{a1} \leftrightarrow AsH^{-1}\;(\text{ascorbate monoanion}) + H^+ \quad (6)$$

$$AsH^{-1}\,(\text{ascorbic acid})\, pK_{a2} \leftrightarrow As\,(\text{ascorbate dianion}) + H^+ \quad (7)$$

In the equilibrium stage, the values of pK_{a1} and pK_{a2} would be 4.17 and 11.57, respectively (Mukai et al., 1991). The influence of pH on the ascorbic acid reaction has been the subject of several studies (Goia & Matijević, 1999; Luty-błocho et al., 2013; Malassis et al., 2016). At a lower pH, the oxidation potential of L-ascorbic acid is high, such that it takes a long time to reduce the Au^{3+} ions. As the pH increases, the number of L-ascorbic acid molecules gradually deprotonates while the number of As^{2-} species increases. This As^{2-} has a high reduction potential and can efficiently reduce the Au^{3+} ions. These findings were further clarified by measuring the redox potential while changing the pH of the L-ascorbic acid solution. The obtained results show that the redox rate changes from negative to positive as the pH increases. This result indicates that the reduction of the Au^{3+} ions by the L-ascorbic acid is considerable at higher pH values.

Limitations of electrospray process

The corona discharge is a major limitation associated with the electrospray process (Saallah et al., 2014). In the present study, the electrospray was hindered, resulting in an unstable electrospray, when the flow rate exceeded the limit of 2 mL/h and the metal ion (Au^{3+}) precursor concentration exceeded the limit of 2 mM. Increasing the flow rate, metal-ion concentration, and applied voltage resulted in an excessive current flowing through the jet, causing

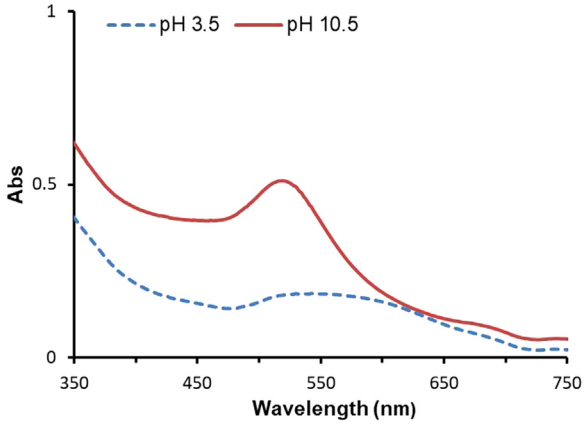

Fig. 8. UV–vis spectra of electrosprayed GNPs produced by L-ascorbic acid solutions with pH values of 3.5 and 10.5.

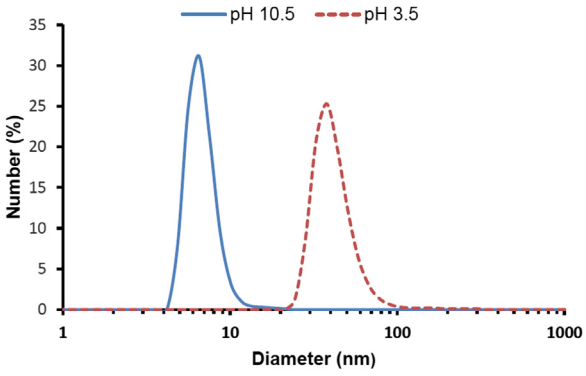

Fig. 9. DLS size distribution of electrosprayed GNPs produced using L-ascorbic acid with pH values of 3.5 and 10.5.

a corona discharge (Zeleny, 1914). However, the corona discharge in the electrospray process can be mitigated by optimizing the vicinity of the electrospray using insulating gases such as CO_2, N_2, or Ar, or feeding inert gases along with the electrospray (Goia & Matijević, 1999; Rosell-Llompart & Fernández de la Mora, 1994; Tang & Gomez, 1994). The electric charge on the droplets is insulated by these inert gases, preventing the draining of the electric current to the air.

Conclusion

GNPs were synthesized in an electrospray-assisted system via mist and liquid reactions. The mean nanoparticle size, morphology, and PDI were controlled by manipulating electrospray droplet size and concentration of the electrospray precursor (Au^{3+}). In the electrospray process, the precursor solution was transformed into

nanometric droplets whereby the droplet size increased with the flow rate and as the metal-ion concentration decreased. Meanwhile, the mean diameter of the GNPs in the liquid reactor decreased as the flow rate increased. This response implied that increasing the size of the droplets at a higher flow rate led to a higher nucleation rate relative to the formation of smaller AuNPs. Similarly, an increased concentration of the Au^{3+} precursor solution resulted in a decrease in the hydrodynamic particle size. Therefore, a high concentration of electrospray droplets contains large amounts of metal ions for the reaction and stimulates a fast nucleation rate that is dominant over the growth. However, a very high concentration of Au^{3+} precursor solution resulted in a high PDI due to secondary nucleation and seed-mediated growth. Furthermore, monodispersed and smaller GNPs were produced in the presence of PVP, whereas highly aggregated and larger AuNPs were produced in the non-PVP samples, indicating that the passive stabilizer controlled the AuNP size in the electrospray process. The results of this study suggest that GNPs with preferable properties could be synthesized using an electrospray-based chemical reduction method with a minimum protocol. An electrospray system for GNPs production could be developed for use with high concentrations of precursor solutions and high flow rates. The results have the potential to be used as the basis for the future scaling up of nanoparticle production, given the high flexibility and easy operation of the system.

Declaration of interests

The authors declare that they have no known competing financial interests or personal relationships that could have appeared to influence the work reported in this paper.

Acknowledgment

The authors acknowledge the financial support of the Ministry of Higher Education, Malaysia (MOHE) in the form of a Fundamental Research Grant Scheme (grant no.: FRGS/1/2018/STG05/UiTM/02/3).

References

Alex, S., & Tiwari, A. (2015). Functionalized gold nanoparticles: Synthesis, properties and applications—A review. *Journal of Nanoscience and Nanotechnology*, *15*(3), 1869–1894.

Amendola, V., Pilot, R., Frasconi, M., Maragò, O. M., & Iatì, M. A. (2017). Surface plasmon resonance in gold nanoparticles: A review. *Journal of Physics: Condensed Matter*, *29*(20). Article 203002.

Bandulasena, M. V., Vladisavljević, G. T., Odunmbaku, O. G., & Benyahia, B. (2017). Continuous synthesis of PVP stabilized biocompatible gold nanoparticles with a controlled size using a 3D glass capillary microfluidic device. *Chemical Engineering Science*, *171*, 233–243.

Barrero, A., & Loscertales, I. G. (2007). Micro- and nanoparticles via capillary flows. *Annual Review of Fluid Mechanics*, *39*(1), 89–106.

Brust, M., Walker, M., Bethell, D., Schiffrin, D. J., & Whyman, R. (1994). Synthesis of thiol-derivatised gold nanoparticles in a two-phase liquid–liquid system. *Journal of the Chemical Society, Chemical Communications*, *7*, 801–802.

D'Souza, S. L., Pati, R. K., & Kailasa, S. K. (2014). Ascorbic acid functionalized gold nanoparticles as a probe for colorimetric and visual read-out determination of dichlorvos in environmental samples. *Analytical Methods*, *6*(22), 9007–9014.

Dhumale, V. A., Gangwar, R. K., Datar, S. S., & Sharma, R. B. (2012). Reversible aggregation control of polyvinylpyrrolidone capped gold nanoparticles as a function of pH. *Materials Express*, *2*(4), 311–318.

Dykman, L. A., & Khlebtsov, N. G. (2011). Gold nanoparticles in biology and medicine: Recent advances and prospects. *Acta Naturae*, *3*(2), 34–55.

Fernández de la Mora, J. (2007). The fluid dynamics of taylor cones. *Annual Review of Fluid Mechanics*, *39*(1), 217–243.

Goia, D., & Matijević, E. (1999). Tailoring the particle size of monodispersed colloidal gold. *Colloids and Surfaces A: Physicochemical and Engineering Aspects*, *146*(1–3), 139–152.

Gomez, A., & Tang, K. (1994). Charge and fission of droplets in electrostatic sprays. *Physics of Fluids*, *6*(1), 404–414.

Haiss, W., Thanh, N. T. K., Aveyard, J., & Fernig, D. G. (2007). Determination of size and concentration of gold nanoparticles from UV–vis spectra — Supporting info. *Analytical Chemistry*, *79*(11), 4215–4221.

Halimi, S. U., Abd Hashib, S., Abu Bakar, N. F., Ismail, S. N., Nazli Naim, M., Abd Rahman, N., & Krishnan, J. (2018). Formation of sol gel dried droplets of carbon doped titanium dioxide (TiO_2) at low temperature via electrospraying. *IOP Conference Series: Materials Science and Engineering*, *358*(1).

Halimi, S. U., Abu Bakar, N. F., Ismail, S. N., Hashib, S. A., & Naim, M. N. (2014). Electrospray deposition of titanium dioxide (TiO_2) nanoparticles. *AIP Conference Proceedings*, *1586*(February), 57–62.

Hartman, R. P. A., Brunner, D. J., Camelot, D. M. A., Marijnissen, J. C. M., & Scarlett, B. (2000). Jet break-up in electrohydrodynamic atomization in the cone-jet mode. *Journal of Aerosol Science*, *31*(1), 65–95.

Hogan, C. J., Yun, K. M., Chen, D., Lenggoro, I. W., Biswas, P., & Okuyama, K. (2007). Controlled size polymer particle production via electrohydrodynamic atomization. *Colloids and Surfaces A: Physicochemical and Engineering Aspects*, *311*(1–3), 67–76.

Homberger, M., & Simon, U. (2010). On the application potential of gold nanoparticles in nanoelectronics and biomedicine. *Philosophical Transactions of the Royal Society A: Mathematical, Physical and Engineering Sciences*, *368*(1915), 1405–1453.

Hoppe, C. E., Lazzari, M., Pardiñas-Blanco, I., & López-Quintela, M. A. (2006). One-step synthesis of gold and silver hydrosols using poly(*N*-vinyl-2-pyrrolidone) as a reducing agent. *Langmuir*, *22*(16), 7027–7034.

Kimling, J., Maier, M., Okenve, B., Kotaidis, V., Ballot, H., & Plech, A. (2006). Turkevich method for gold nanoparticle synthesis revisited. *The Journal of Physical Chemistry B*, *110*(32), 15700–15707.

Lenggoro, I. W., Xia, B., Okuyama, K., & de la Mora, J. F. (2002). Sizing of colloidal nanoparticles by electrospray and differential mobility analyzer methods. *Langmuir*, *18*(12), 4584–4591.

Lince, F., Marchisio, D. L., & Barresi, A. A. (2008). Strategies to control the particle size distribution of poly-ε-caprolactone nanoparticles for pharmaceutical applications. *Journal of Colloid and Interface Science*, *322*(2), 505–515.

Lohse, S. E., Eller, J. R., Sivapalan, S. T., Plews, M. R., & Murphy, C. J. (2013). A simple millifluidic benchtop reactor system for the high-throughput synthesis and functionalization of gold nanoparticles with different sizes and shapes. *ACS Nano*, *7*(5), 4135–4150.

Luo, C., Okubo, T., Nangrejo, M., & Edirisinghe, M. (2015). Preparation of polymeric nanoparticles by novel electrospray nanoprecipitation. *Polymer International*, *64*(2), 183–187.

Luty-błocho, M., Pacławski, K., Wojnicki, M., & Fitzner, K. (2013). The kinetics of redox reaction of gold(III) chloride complex ions with L-ascorbic acid. *Inorganica Chimica Acta*, *395*, 189–196.

Mafuné, F., Kohno, J., Takeda, Y., Kondow, T., & Sawabe, H. (2001). Formation of gold nanoparticles by laser ablation in aqueous solution of surfactant. *The Journal of Physical Chemistry B*, *105*(22), 5114–5120.

Malassis, L., Dreyfus, R., Murphy, R. J., Hough, L. A., Donnio, B., & Murray, C. B. (2016). One-step green synthesis of gold and silver nanoparticles with ascorbic acid and their versatile surface post-functionalization. *RSC Advances*, *6*(39), 33092–33100.

Mukai, K., Nishimura, M., & Kikuchi, S. (1991). Stopped-flow investigation of the reaction of vitamin C with tocopheroxyl radical in aqueous Triton X-100 micellar solutions. The structure-activity relationship of the regeneration reaction of tocopherol by vitamin C. *Journal of Biological Chemistry*, *266*(1), 274–278.

Naim, M. N., Jaafar, A. R., Abu Bakar, N. F., Baharuddin, A. S., Kadir Basha, R., & Lenggoro, I. W. (2015). Deposition of nanostructures derived from electrostatically stabilised TiO_2 aqueous suspension onto a biocomposite. *Advanced Powder Technology*, *26*(2), 362–367.

Pacławski, K., Jaworski, W., Streszewski, B., & Fitzner, K. (2011). In V. Starov, & K. Procházka (Eds.), *Trends in colloid and interface science XXIV*. Berlin Heidelberg: Springer. Issue January 2015.

Papp, S., Patakfalvi, R., & Dekany, I. (2007). Formation and stabilization of noble metal nanoparticles. *Croatica Chemica Acta*, *80*(3–4), 493–502.

Quintanilla, A., Valvo, M., Lafont, U., Kelder, E. M., Kreutzer, M. T., & Kapteijn, F. (2010). Synthesis of anisotropic gold nanoparticles by electrospraying into a reductive-surfactant solution. *Chemistry of Materials*, *22*(5), 1656–1663.

Ramakrishna, S., & Sreedar, R. (2013). Electrosprayed nanoparticles for drug delivery and pharmaceutical applications. *Biomatter*, *3*(3), Article e24281.

Rosell-Llompart, J., & Fernández de la Mora, J. (1994). Generation of monodisperse droplets 0.3 to 4 μm in diameter from electrified cone-jets of highly conducting and viscous liquids. *Journal of Aerosol Science*, *25*(6), 1093–1119.

Saallah, S., Naim, N. N., Mokhtar, M. N., Abu Bakar, N. F., Gen, M., & Lenggoro, W. W. (2014). Transformation of cyclodextrin glucanotransferase (CGTase) from aqueous suspension to fine solid particles via electrospraying. *Enzyme and Microbial Technology*, *64–65*, 52–59.

Smith, D. P. H. (1986). The electrohydrodynamic atomization of liquids. *IEEE Transactions on Industry Applications*, *IA-22*(3), 527–535.

Soliwoda, K., Rosowski, M., Tomaszewska, E., Tkacz-Szczesna, B., Celichowski, G., Psarski, M., & Grobelny, J. (2015). Synthesis of monodisperse gold nanoparticles via electrospray-assisted chemical reduction method in cyclohexane. *Colloids and Surfaces A: Physicochemical and Engineering Aspects*, *482*, 148–153.

Stratakis, M., & Garcia, H. (2012). Catalysis by supported gold nanoparticles: Beyond aerobic oxidative processes. *Chemical Reviews*, *112*, 4469–4506.

Sugano, K., Uchida, Y., Ichihashi, O., Yamada, H., Tsuchiya, T., & Tabata, O. (2010). Mixing speed-controlled gold nanoparticle synthesis with pulsed mixing microfluidic system. *Microfluidics and Nanofluidics*, *9*(6), 1165–1174.
Sztandera, K., Gorzkiewicz, M., & Klajnert-Maculewicz, B. (2019). Gold nanoparticles in cancer treatment. *Molecular Pharmaceutics*, *16*(1), 1–23.
Tang, K., & Gomez, A. (1994). Generation by electrospray of monodisperse water droplets for targeted drug delivery by inhalation. *Journal of Aerosol Science*, *25*(6), 1237–1249.
Thanh, N. T. K., Maclean, N., & Mahiddine, S. (2014). Mechanisms of nucleation and growth of nanoparticles in solution. *Chemical Reviews*, *114*(15), 7610–7630.
Thompson, D. T. (2007). Using gold nanoparticles for catalysis. *Nano Today*, *2*(4), 40–43.
Tran, M., DePenning, R., Turner, M., & Padalkar, S. (2016). Effect of citrate ratio and temperature on gold nanoparticle size and morphology. *Materials Research Express*, *3*(10), 1–10.
Tyagi, H., Kushwaha, A., Kumar, A., & Aslam, M. (2016). A facile pH controlled citrate-based reduction method for gold nanoparticle synthesis at room temperature. *Nanoscale Research Letters*, *11*(1), 362.
Wortmann, A., Kistler-Momotova, A., Zenobi, R., Heine, M. C., Wilhelm, O., & Pratsinis, S. E. (2007). Shrinking droplets in electrospray ionization and their influence on chemical equilibria. *Journal of the American Society for Mass Spectrometry*, *18*(3), 385–393.
Yeh, Y.-C., Creran, B., & Rotello, V. M. (2012). Gold nanoparticles: preparation, properties, and applications in bionanotechnology. *Nanoscale*, *4*(6), 1871–1880.
Zeleny, J. (1914). The electrical discharge from liquid points, and a hydrostatic method of measuring the electric intensity at their surfaces. *Physical Review*, *3*(2), 69–91.
Zolkepali, N. K., Abu Bakar, N. F., Naim, M. N., Anuar, N., & Abu Bakar, M. R. (2014). Nanoparticle preparation of Mefenamic acid by electrospray drying. *AIP Conference Proceedings*, *1586*(February), 113–118.
Zolkepali, N. K., Abu bakar, N. F., Naim, M. N., Anuar, N., Kamalul Aripin, N. F., Abu Bakar, M. R., Lenggoro, I. W., & Kamiya, H. (2018). Formation of fine and encapsulated mefenamic acid form I particles for dissolution improvement via electrospray method. *Particulate Science and Technology*, *36*(3), 298–307.
Zong, R., Wang, X., Shi, S., & Zhu, Y. (2014a). Kinetically controlled seed-mediated growth of narrow dispersed silver nanoparticles up to 120 nm: Secondary nucleation, size focusing, and Ostwald ripening. *Physical Chemistry Chemical Physics*, *16*(9), 4236.
Zong, R., Wang, X., Shi, S., & Zhu, Y. (2014b). Kinetically controlled seed-mediated growth of narrow dispersed silver nanoparticles up to 120 nm: Secondary nucleation, size focusing, and Ostwald ripening. *Journal of the Chemical Society Faraday Transactions*, *16*(9), 4236–4241.